PREDICTION AND OPTIMIZATION OF TIG WELDING PROCESS PARAMETERS OF AISI 317L STAINLESS STEEL PLATES USING RESPONSE SURFACE METHODOLOGY

Abstract

The quality of welds is greatly influenced by the weld bead geometry and mechanical-metallurgical properties of the welded joint which have a direct relationship with the type of welding process being used and its input process parameters such as welding current, gas flow rate, arc voltage, travel speed, etc. In this study, the prediction and optimization of tungsten inert gas (TIG) welding input parameters for achieving maximum tensile strength of 317L stainless steel is investigated. The experimental strategy to determine the impact of process parameters on tensile strength has been developed using a central composite design of response surface methodology. Two levels of welding input parameters were used to create the square butt joint configuration. The results indicate that gas flow rate has a greater influence on tensile strength followed by welding current. The model F-value of 18.19 at a P value of 0.0026 for the tensile strength showed the significance of the model employed. The optimal tensile strength of 618.627 MPa was observed at a current of 150 A, travel speed at 15.69 cm/min, and gas flow rate at 8.96 l/min.

Keywords: Tungsten Inert Gas welding, Tensile strength, Central Composite Design, Analysis of variance, Response Surface Methodology.

1. Introduction

The grade 317L austenitic stainless steel is an important material that is frequently used in industries like automobile, thermal power plants, nuclear power plants, chemical, and pharmaceutical industries as a result of its high strength, weldability, higher corrosion resistance, high ductility, and formability. Amongst the various types of welding methods, Tungsten Inert Gas (TIG) welding is the most frequently used for welding austenitic stainless steel [1]. Welding input parameters play a major role in determining the mechanical properties such as tensile strength, hardness, etc of the welded joint. As a result, the careful selection of the welding input parameters and their levels is very important to obtain optimal mechanical properties [2, 3, 4]. In order to postulate the relationships between the input parameters and output variables, various optimization techniques can be used to determine the desired output responses. The response surface methodology (RSM) is one of the most frequently used statistical optimization methods [5, 6, 7]. Koleva [8] used the response surface method to determine the connection between the performance characteristics of weld width, weld depth, and thermal efficiency and their influencing factors (beam power, welding velocity, focus position, beam focusing current, and sample surface distance) for austenitic stainless steel. Kiaee et al., [9] used response surface methodology for the optimization of TIG welding process parameters for the joining of A516-Gr70 carbon steels. The optimization of CO2 welding process parameters for weld bead penetration of mild steel using RSM was reported by [10]. Weld bead penetration was correlated mathematically with welding process parameters like voltage, travel speed, and welding current. The optimal values for the different input parameters were recorded as 20V for the arc voltage, 40cm/min for the travel speed, 230A for the welding current, and 0.88mm for the maximum bead penetration [11, 12]. Thermal efficiency optimization was used to identify the best welding conditions. An attempt has been made in this paper, to optimize the tensile strength properties of AISI 317L stainless steel plates using the response surface methodology.

2. METHODOLOGY

AISI 317L stainless steel plates of size 100 mm by 45mm by 5mm and ER 317L austenitic steel have been chosen as our base material and filler metal respectively for this study. In Table 1, the chemical composition of the base material is presented. The mechanical properties of the base material are as follows: tensile strength 595MPa, yield strength 260MPa, Modulus of elasticity 200GPa, and Rockwell hardness B 85. The most significant parameters that influence the mechanical properties of tungsten inert gas welded joints are obtained through an extensive literature review. The identified important input parameters are welding current, travel speed, and gas flow rate. The selected input parameters and their levels are shown in Table 2. The central composite design (CCD) of experiments which is the most frequently used method amongst the other types of RSM methods, was chosen for this study because of its flexibility, high efficiency and ability to be run in sequence. Using the Design expert software version 8.0.6, a central composite design matrix of fifteen (15) experimental runs was developed as shown in Table 3. The experiment was performed in three stages. In the first stage, the metal plate edges were prepared and taken for forming the welded joint as shown in the specimen sample shown in Figure 1. The second stage was the welding process and the joint formation using the design matrix. The third stage was the testing and recording of the response (tensile strength). With the fifteen (15) experimental runs generated in Table 3, fifteen coupons were welded using the tungsten inert gas welding method and thereafter allowed to cool naturally in the open air, with all necessary precautions observed. The welded plates were sliced in the transverse section as shown in Figure 2 to obtain samples for the tensile test.

Table 1: Chemical composition of grade 317L stainless steel

Element	Content (%)
Iron	Balance
Chromium	18-20
Nickel	11-15
Molybdenum	3-4
Manganese	2
Silicon	1
Phosphorus	0.045
Carbon	0.03
Sulphur	0.03

Table 2: TIG welding parameters and their levels

Parameter	Units	Symbol	Coded Value Low (-1)	Coded Value High (+1)
Welding Current	Amp	A	100	150
Travel speed	cm	B	12	18
Gas flow rate	l/min	C	6	12

Table 3: Central composite design matrix of welding parameters

		Factor 1	Factor 2	Factor 3
Std	Run	A:Welding current	B:Travel speed	C:Gas flow rate
		Amp	cm	l/min
1	10	100	12	9
2	12	150	12	9
3	15	100	18	9
4	7	150	18	9
5	14	100	15	6
6	16	150	15	6
7	3	100	15	12
8	8	150	15	12
9	4	125	12	6
10	13	125	18	6
11	5	125	12	12
12	1	125	18	12
13	2	125	15	9
14	17	125	15	9
15	9	125	15	9

2.1 Tensile Strength Test

The samples for the tensile test were prepared by milling the bottom and top surfaces to remove all surface anomalies by ASTM E8 specification. The tensile test was carried out on all fifteen welded specimens using the universal testing machine.

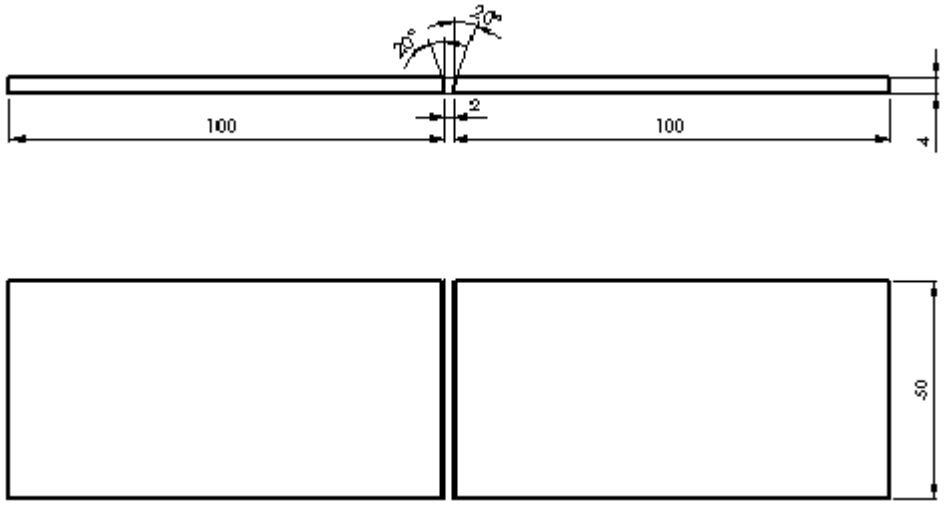

Fig. 1: Sample of specimen

Fig. 2: Welded specimen

The model of the response surface methodology is given by Equation (1).

$$Y = b_0 + \sum_{i=1}^{K}(b_i x_i) + \sum_{i=1}^{k}(b_{ii} x_i^2) + \sum_{i=1}^{K}(b_{ij} x_i x_j) + \varepsilon \quad (1)$$

where $Y = response\ variables\ or\ dependent\ variables$

$x_i = predicted\ variables\ or\ independent\ variables$

$b_0 = model\ constant$

$\varepsilon = random\ error$

parameters b_i, b_{ii}, b_{ij} are known as regression coefficient where $i = 1, 2, 3 \ldots k\ and\ j = 1, 2, 3, \ldots k$.

3. Result and Discussion

The randomized design matrix of the welding parameters (welding current, travel speed, and gas flow rate) with the experimental results of the response factor (tensile strength) presented in Table 4 were obtained from design expert 8.0.6. It is observed from Table 4 that sample number 14 had the highest tensile strength (625.45 MPa) while sample number 7 depicted the lowest tensile strength of 584.61 MPa.

Table 4: Central composite design of the experiment

		Factor 1	Factor 2	Factor 3	Response 1
Std	Run	A:Welding current (A)	B:Travel speed (cm)	C:Gas flow rate (l/min)	Tensile strength (MPa)
1	10	100	12	9	601.11

2	12	150	12	9	606.42
3	15	100	18	9	597.48
4	7	150	18	9	617.37
5	14	100	15	6	608.26
6	16	150	15	6	601.91
7	3	100	15	12	584.61
8	8	150	15	12	599.69
9	4	125	12	6	610.15
10	13	125	18	6	602.24
11	5	125	12	12	592.42
12	1	125	18	12	594.88
13	2	125	15	9	622.42
14	17	125	15	9	625.45
15	9	125	15	9	622.85

ANOVA test was done to ascertain the significance of the model and to also determine the contribution of each of the welding process parameters on the response (tensile strength). When the F-value is large and the p-value is less than 0.05%, it signifies the absence of external influence on the variance and also confirms the significance of the model [13]. Table 5 shows the analysis of variance results for validating the model significance in optimizing tensile strength. The Model F-value of 18.19 implies the model is significant. There is only a 0.26% chance that a "Model F-Value" this large could occur due to noise. Values of "Prob > F" less than 0.0500 indicate model terms are significant. From observation of Table 5, A, C, AC, A2, B2, and C2 are significant model terms. The lack of fit value of 6.74 implies the lack of fit is not significant which is desirable as we want the model to fit. The ANOVA result shows that gas flow rate is the most significant parameter that affects the tensile strength followed by welding current. Travel speed has the least effect on tensile strength.

Table 5: ANOVA result for validating the model significance

Analysis of variance table [Partial sum of squares - Type III]						
	Sum of		Mean	F	p-value	
Source	Squares	df	Square	Value	Prob > F	Remarks
Model	1956.168	9	217.3521	18.19057	0.0026	significant
A-Current	143.9056	1	143.9056	12.04371	0.0178	significant
B-travel speed	0.437112	1	0.437112	0.036583	0.8558	Not significant
C-gas flow rate	324.6152	1	324.6152	27.16762	0.0034	Significant
AB	53.1441	1	53.1441	4.447723	0.0887	Not significant
AC	114.8112	1	114.8112	9.608753	0.0269	Significant
BC	26.88423	1	26.88423	2.249988	0.1939	Not significant
A^2	343.2433	1	343.2433	28.72664	0.0030	Significant
B^2	256.6154	1	256.6154	21.4766	0.0057	Significant
C^2	865.9337	1	865.9337	72.47151	0.0004	Significant
Residual	59.74304	5	11.94861			
Lack of Fit	54.36777	3	18.12259	6.742955	0.1319	Not significant
Pure Error	5.375267	2	2.687633			
Cor Total	2015.911	14				

Table 6: Goodness of fit statistics

Std. Dev.	3.456676		R-Squared	0.970364
Mean	605.8173		Adj R-Squared	0.91702
C.V. %	0.570581		Pred R-Squared	0.562491
PRESS	881.9787		Adeq Precision	14.50011

The coefficient of determination (R-Squared) of 0.9703 as observed in Table 6 shows the strength of response surface methodology and its ability to predict the optimal values of the selected variables that will maximize the tensile strength. The Coefficient of determination (R-Squared) of 0.9703 indicates that 97% of the total variations as in the case of the response (tensile strength) can be explained by the model. The value of the adjusted coefficient of determination Adj. R-Squared value of 0.917 indicates a model with 91.7% reliability. Adequate precision measures the signal-to-noise ratio. A ratio greater than 4 is desirable. An adequate precision value of 14.5 as observed indicates an adequate signal, indicating that the model can be used to maximize the tensile strength.

Optimal equations based on coded variables

The best equation that depicts the individual effects and combined interactions of the chosen variables against the considered approach (tensile strength) in terms of coded factors is provided by equation (2)

$$Tensile\ strength = 623.5733 + 4.2413A + 0.2338B - 6.37C + 3.645AB + 5.3575AC + 2.5925BC - 9.6417A^2 - 8.3367B^2 - 15.3142C^2 \quad (2)$$

where $A, B\ and\ C$ represents welding current, travel speed and gas flow rate respectively.

The diagnostics case statistics which shows the observed values of tensile strength against their predicted values is presented in Tables 7.

Table 7 Experimental and predicted tensile strength values

Standard Order	Actual Value	Predicted Value	Residual	Leverage	Internally Studentized Residual	Externally Studentized Residual	Fitted Value DFFITS	Cook's Distance
1	601.11	604.765	-3.655	0.75	-2.11475	** -5.82	* -10.08	* 1.34
2	606.42	605.9575	0.4625	0.75	0.267598	0.24108	0.417562	0.021483
3	597.48	597.9425	-0.4625	0.75	-0.2676	-0.24108	-0.41756	0.021483
4	617.37	613.715	3.655	0.75	2.114748	** 5.82	* 10.08	* 1.34
5	608.26	606.1038	2.15625	0.75	1.247586	1.344617	* 2.33	0.466941
6	601.91	603.8713	-1.96125	0.75	-1.13476	-1.17791	* -2.04	0.386305
7	584.61	582.6488	1.96125	0.75	1.134761	1.177909	* 2.04	0.386305
8	599.69	601.8463	-2.15625	0.75	-1.24759	-1.34462	* -2.33	0.466941
9	610.15	608.6513	1.49875	0.75	0.867163	0.841466	1.457463	0.225591
10	602.24	603.9338	-1.69375	0.75	-0.97999	-0.97517	-1.68904	0.288113
11	592.42	590.7263	1.69375	0.75	0.979988	0.97517	1.689043	0.288113
12	594.88	596.3788	-1.49875	0.75	-0.86716	-0.84147	-1.45746	0.225591
13	622.42	623.5733	-1.15333	0.333333	-0.40864	-0.37176	-0.26287	0.008349
14	625.45	623.5733	1.876667	0.333333	0.664927	0.622907	0.440462	0.022106
15	622.85	623.5733	-0.72333	0.333333	-0.25629	-0.23075	-0.16316	0.003284

Model validation

The residuals' normal probability plot, as seen in Fig. 3, was used to evaluate the model's suitability. From the figure, it can be seen that the residuals follow a straight line, indicating that the errors are normally distributed and that the mathematical relationship has been properly constructed. The comparison of predicted and actual tensile strength values is shown in Fig. 4. The graph indicates that the developed model is suitable. It suggests also that the predicted results and the measured data are in good agreement.

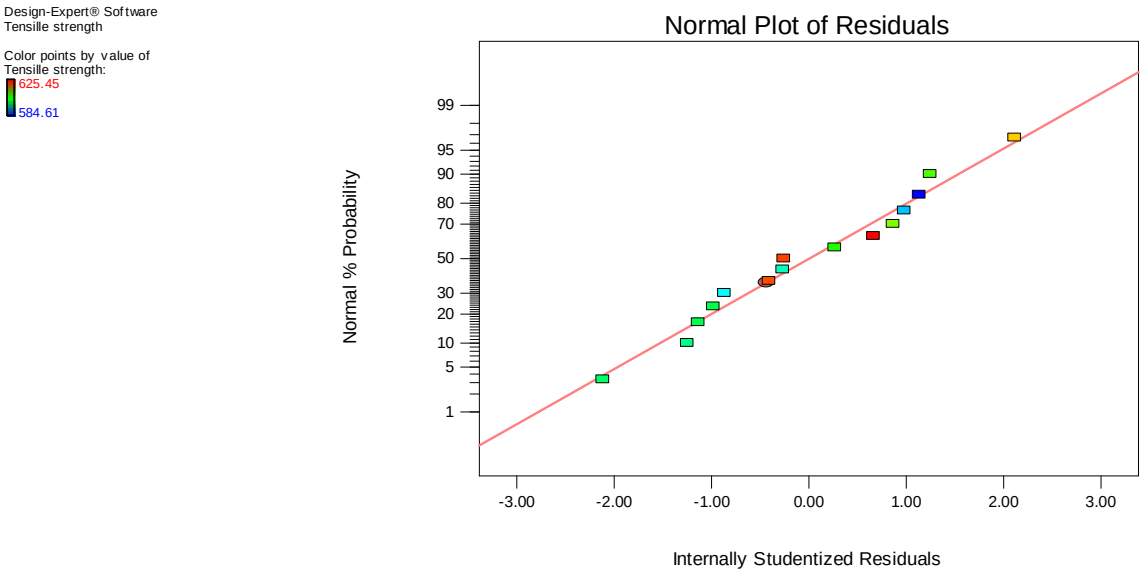

Fig. 3: Residual plot of tensile strength

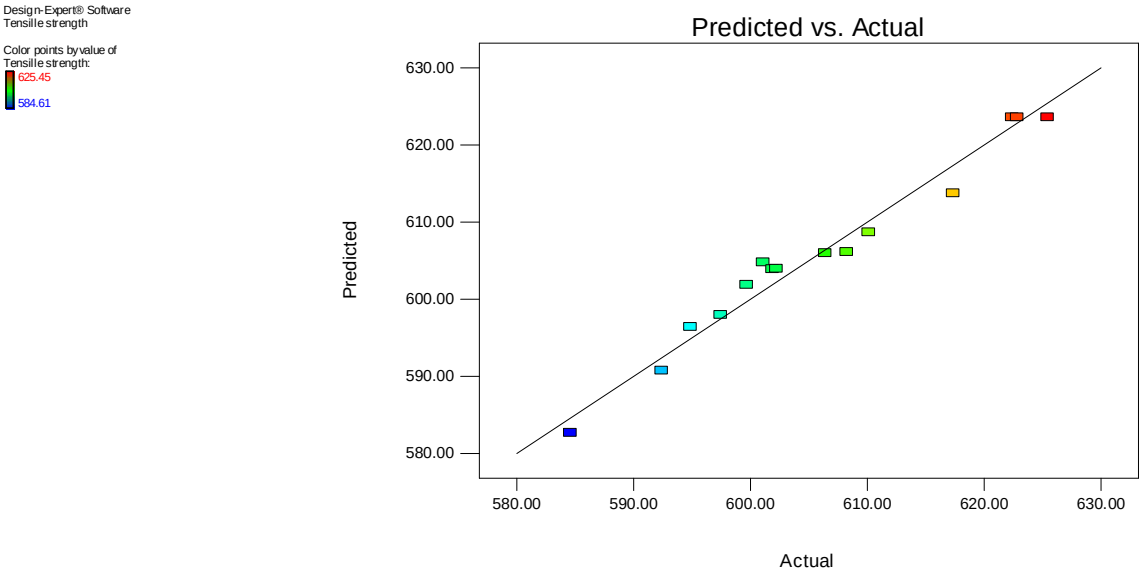

Fig. 4 Predicted vs. actual plot of tensile strength

Effect of the process parameters on tensile strength

The model graphs which show the interaction effects of the process parameters on the measured response (tensile strength) were evaluated using the 3D surface plot as shown in Figs. 5, 6, and 7. Fig. 5 shows the combined effect of travel speed and welding current on tensile strength. It was observed that tensile strength initially increases gradually but decreases with a further increase in the levels of the welding current. The tensile strength is seen to be maximal at average levels of current and travel speed. Fig. 6 shows the joint effect of welding current and gas flow rate on tensile strength. It is observed that tensile strength increases with gas flow rate up to a threshold value and then begins to gradually decrease to its lowest value. Tensile strength is optimum at median values of welding current and gas flow rate. This is because, at a low gas flow rate, there may be contamination leading to weak joint formation. With a further increase in the level of gas flow rate and welding current towards the center value, the tensile strength is observed to have improved. Fig. 7 shows the interaction plot between the gas flow rate and travel speed on the tensile strength. It is seen that the tensile strength is maximum at the median values of gas flow rate and travel speed. When the travel speed is low, the heat input is high and it causes the base metal to overheat which can lead to the formation of poor-strength joints. The most significant parameter of tensile strength is gas flow rate, followed by welding current. The dark colour area on the surface plot as observed in Figs. 5-7 depicts areas of high tensile strength. This agrees with the findings of

[14], who investigated tungsten inert gas welding input parameters to attain the maximum tensile strength of 316L austenitic stainless steel.

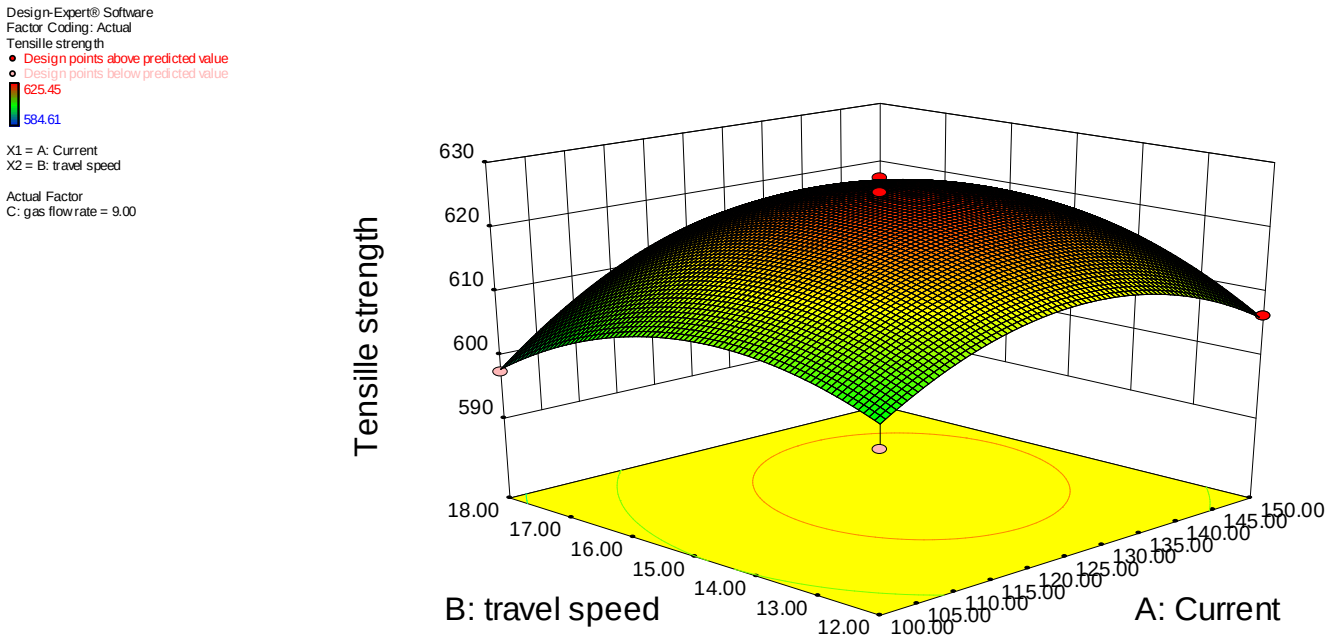

Fig. 5: Effect of travel speed and current on tensile strength

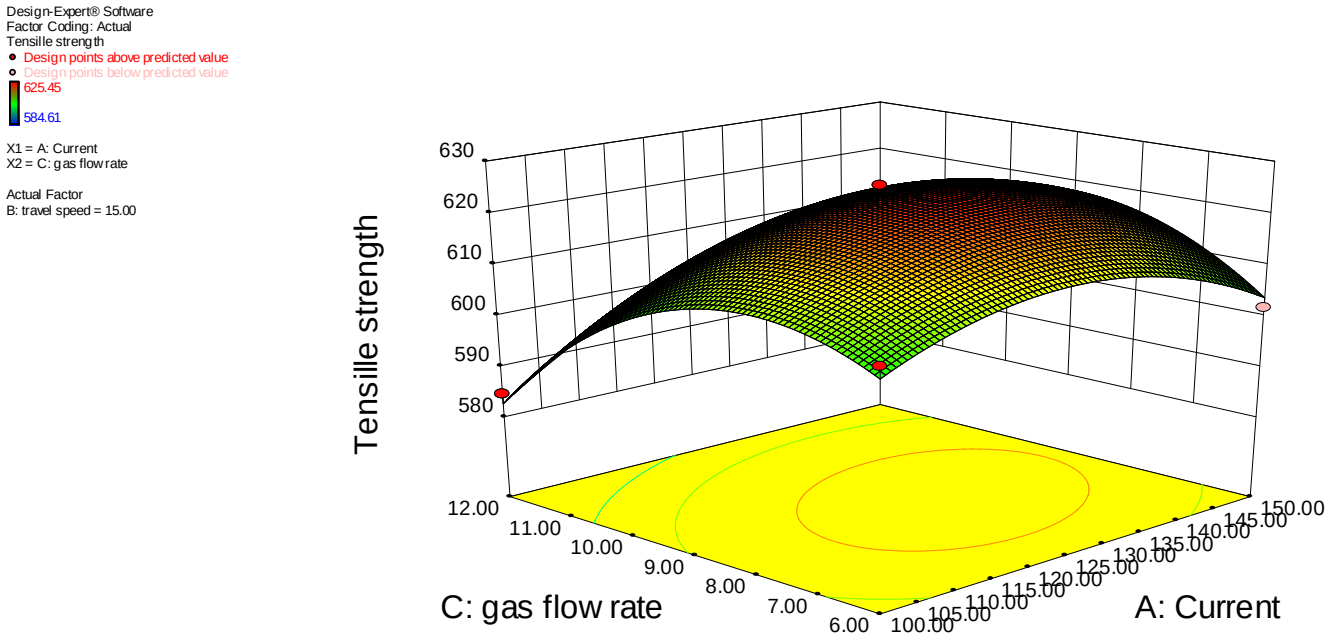

Fig. 6: Effect of gas flow rate and current on tensile strength

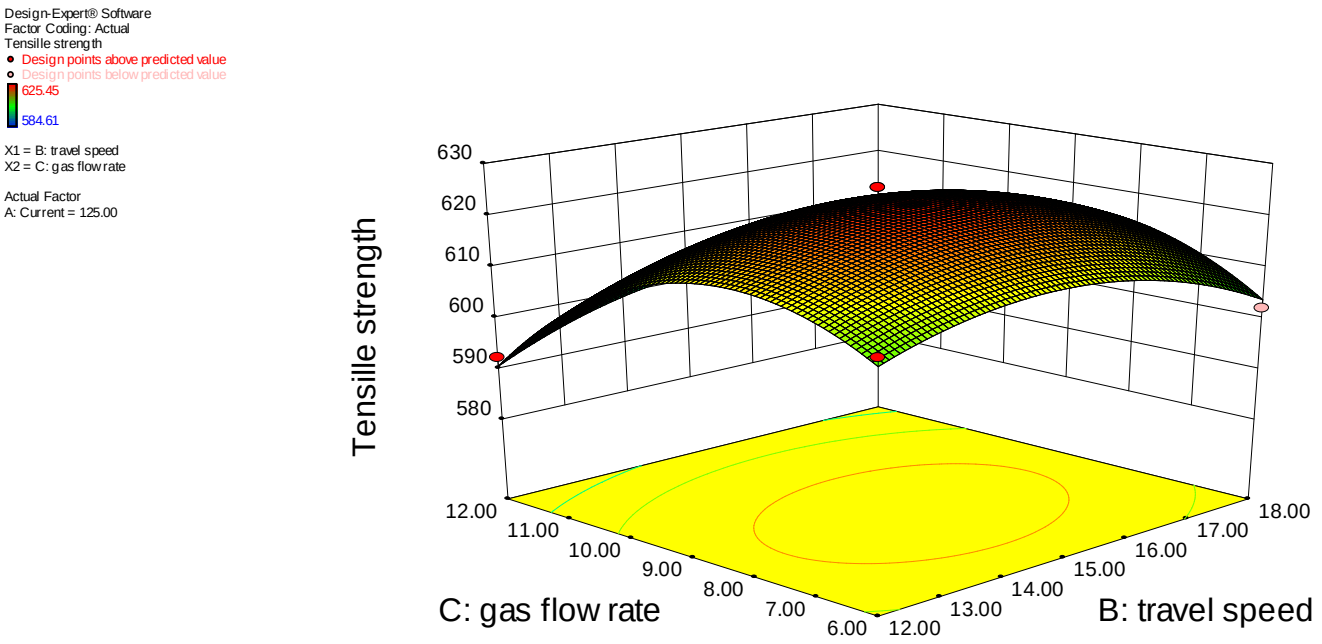

Fig.7: Effect of gas flow rate and travel speed on tensile strength

4. Numerical optimization

Numerical optimization was carried out with the aid of the design expert software to determine the desirability of the overall model. The desirability function analysis is done to obtain optimum parameters settings that will give maximum tensile strength of welded specimens. The optimization results for tensile strength and desirability are shown in Figs. 8-9. The optimum tensile strength 618.627MPa was attained at a welding current of 150A, travel speed of 16.69 cm/min, and gas flow rate of 8.96 l/min. The composite desirability value is 0.913.

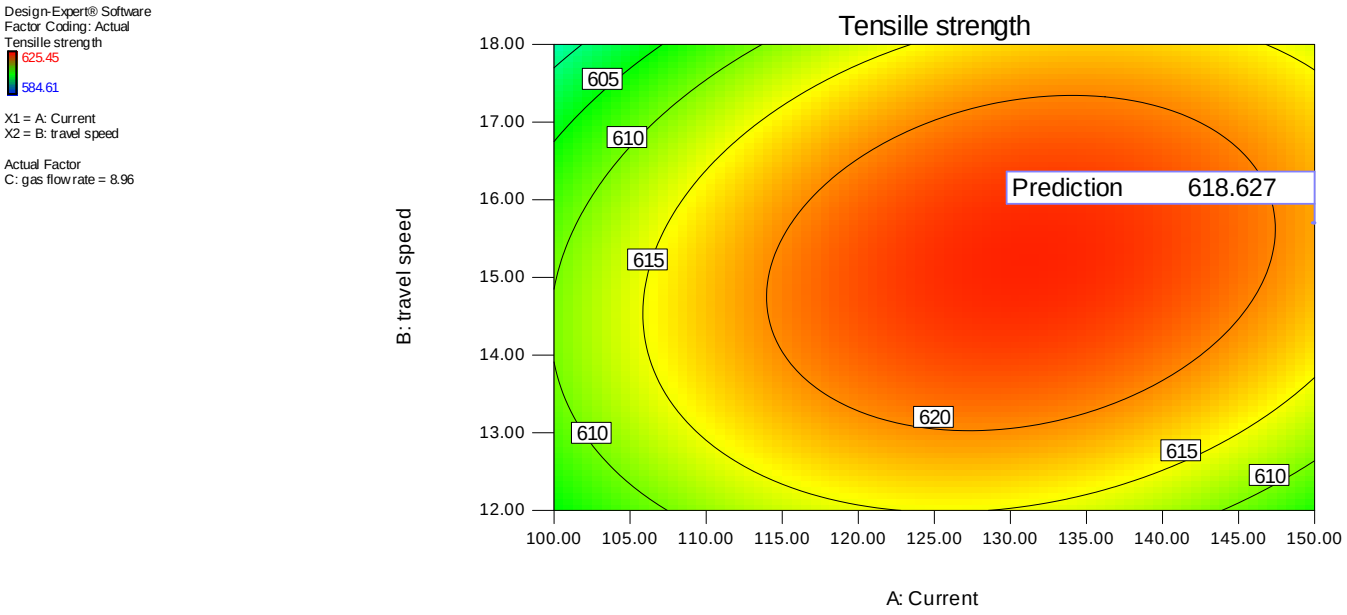

Fig. 8 Optimization results for tensile strength

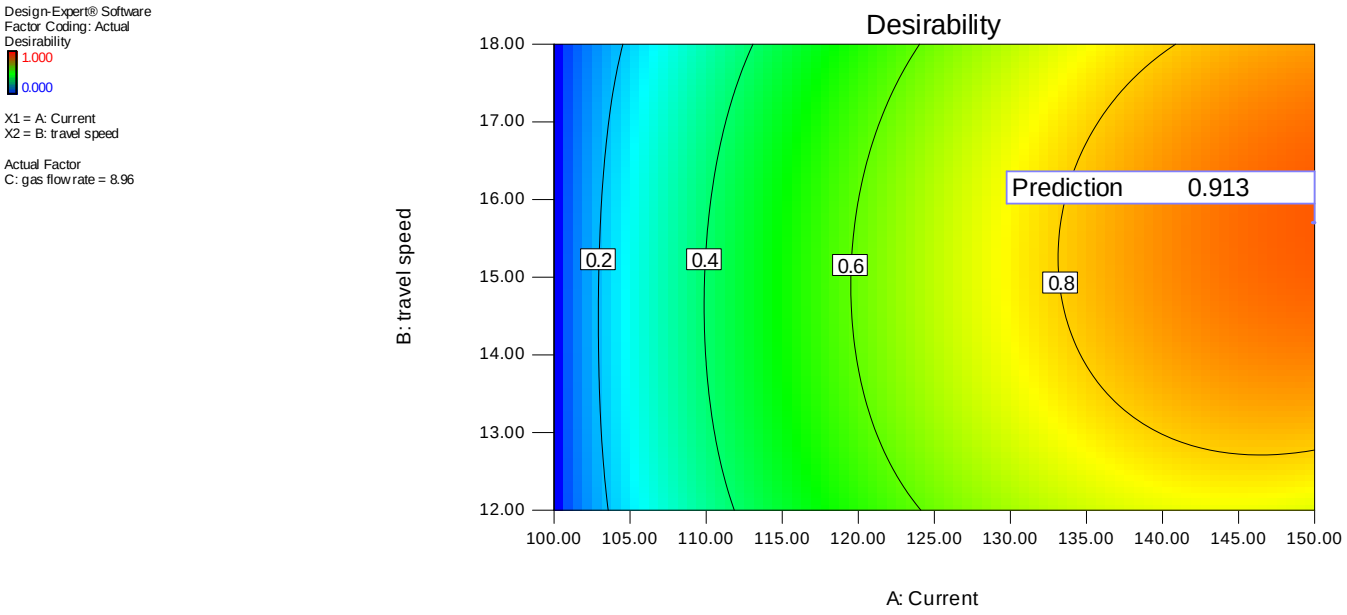

Fig. 9 Optimization results for desirability

4.1 Confirmation test

The result of the confirmation test that was done at optimum conditions of TIG welding process parameters is shown in Table 8. It is observed that the percentage error between the predicted and experimental results is less than 1%. This suggests that the optimized TIG welding process parameters can be taken into consideration to obtain higher tensile strength of 317L stainless steel.

Table 8 Multi-objective optimization results

Welding current (A)	Travel speed (cm/min)	Gas flow rate (l/min)	Tensile strength (MPa)	
150	15.69	8.96	Average Actual	622.73
			Predicted	618.627
			Error %	0.658

5. CONCLUSION

The response surface methodology (RSM) was successfully used to predict optimum process parameters settings for maximum tensile strength of TIG welded plates of AISI 317L stainless steel. The following conclusions are drawn based on the experimental results and analysis: Specimen no. 14 shows the highest tensile strength while specimen no. 7 shows the lowest tensile strength. The ANOVA results show that the most important factor affecting tensile strength is gas flow rate followed by welding current. The experimentally obtained data and the predicted values for tensile strength were compared and the errors were found to be within acceptable levels. The optimum tensile strength of 618.627 MPa is obtained under the welding conditions of current at 150 A, travel speed at 15.69 cm/min, and gas flow rate at 8.96 l/min with a desirability value of 0.913.

REFERENCES

1. Ghosh N., Pal P. K., Nandi G., Rudrapati R. (2018). Parametric optimization of gas metal arc welding process by PCA-based Taguchi method on austenitic stainless steel AISI 316L. Materials Today: Proceedings. Vol. (5), No. 1, 1620 - 1625.
2. Tarng Y. S. and Yang W. H. (1998). Optimization of the weld bead geometry in gas tungsten arc welding by the Taguchi method. The International Journal of Advanced Manufacturing Technology. Vol. (14), No. 8, 549 – 554.
3. Juang S.C. & Y. S. Tarng (2002). Process parameter selection for optimizing the weld pool geometry in the tungsten inert gas welding of stainless steel. Journal of Materials Processing Technology. Vol. (122), No. 1, 33 – 37.
4. Bodkhe S. C. & Dolas D. R. (2018). Optimization of activated tungsten inert gas welding of 304L austenitic stainless steel. Procedia Manufacturing. Vol. (20), 277 – 282.
5. Benyounis K. Y. & Olabi A. G. (2008). Optimization of different welding processes using statistical and numerical approaches – A reference guide. Advances in Engineering Software. Vol. (39), No. 6, 483 – 496.
6. Gunaraj V. & Murugan N. (1999). Application of response surface methodology for predicting weld bead quality in submerged arc welding of pipes. Journal of Materials Processing Technology. Vol. (88), 266 – 275.

7. Kumar A. & Sundarrajan S. (2009). Optimization of pulsed TIG welding process parameters on mechanical properties of AA 5456 Aluminum alloy weldments. Materials and Design. Vol. (30), No. 4, 1288 – 1297.
8. Koleva, E. (2001). Statistical Modelling and Computer Programs for Optimization of the Electron Beam Welding of Stainless Steel" Journal of Vacuum Science and Tech, Vol. 6, pp. 51-57.
9. Kiaee, N. & Aghaie-khafri, M. (2014). Optimization of gas tungsten arc welding process by response surface methodology. Materials and Design. 54. 25–31. 10.1016/j.matdes.2013.08.032.
10. Narayan, K. L., Ramakrishna Ch., Sarcar, M. and Mallikarjuna R K (2014). Optimization of CO2 Welding Process Parameters for Weld Bead Penetration of Mild Steel Using RSM", International Journal of Research in Mechanical Engineering & Technology. Vol. 4, pp 111-115.
11. Kalita K, Burande D, Ghadai RK, Chakraborty S. (2022). Finite Element Modelling, Predictive Modelling and Optimization of Metal Inert Gas, Tungsten Inert Gas, and Friction Stir Welding Processes: A Comprehensive Review. Archives of Computational Methods in Engineering.
12. Pandya D, Badgujar A, Ghetiya N. (2021). A novel perception toward welding of stainless steel by activated TIG welding: a review. Materials and Manufacturing Processes. 36(8):877-903.
13. Juang, S. C. and Tarng, Y. S (2002). "Process Parameters Selection for Optimizing the Weld Pool Geometry in the TIG Welding of Stainless Steel"; Journal of Material Process Technology. pp. 33-37.
14. Moi, Subhas & Pal, Pradip Kumar & Bandyopadhyay, Rudrapati, Ramesh. (2018). Determination of Tungsten Inert Gas Welding Input Parameters to Attain Maximum Tensile Strength of 316L Austenitic Stainless Steel. Journal of Mechanical Engineering. 68. 231-248. 10.2478/scjme-2018-0037.